Representation of Water Table Dynamics in a Land Surface Scheme. Part II: Subgrid Variability

PAT J.-F. YEH* AND ELFATIH A. B. ELTAHIR

Ralph M. Parsons Laboratory, Department of Civil and Environmental Engineering, Massachusetts Institute of Technology, Cambridge, Massachusetts

ABSTRACT

A lumped unconfined aquifer model has been developed and interactively coupled to a land surface scheme in a companion paper. Here, the issue of the representation of subgrid variability of water table depths (WTDs) is addressed. A statistical–dynamical (SD) approach is used to account for the effects of the unresolved subgrid variability of WTD in the grid-scale groundwater runoff. The dynamic probability distribution function (PDF) of WTD is specified as a two-parameter gamma distribution based on observations. The grid-scale groundwater rating curve (i.e., aquifer storage–discharge relationship) is derived statistically by integrating a point groundwater runoff model with respect to the PDF of WTD. Next, a mosaic approach is utilized to account for the effects of subgrid variability of WTD in the grid-scale groundwater recharge. A grid cell is categorized into different subgrids based on the PDF of WTD. The grid-scale hydrologic fluxes are computed by averaging all of the subgrid fluxes weighted by their fractions. This new methodology combines the strengths of the SD approach and the mosaic approach. The results of model testing in Illinois from 1984 to 1994 indicate that the simulated hydrologic variables (soil saturation and WTD) and fluxes (evaporation, runoff, and groundwater recharge) agree well with the observations. Because of the paucity of the large-scale observations on WTD, the development of a practical parameter estimation procedure is indispensable before the global implementation of the developed scheme of water table dynamics in climate models.

1. Introduction

A natural land surface usually exhibits considerable variability in vegetation cover, topography, soil characteristics (e.g., soil texture, hydraulic properties, and organic content), and water table depth (WTD). These land surface characteristics may vary over a wide spectrum of spatial scales. Moreover, the climate forcing (e.g., precipitation, radiation, temperature, etc.) may also vary over the unresolved spatial scales of typical atmospheric models. Because of the nonlinear nature of land surface processes, these variabilities can significantly affect the exchanges of momentum, water, and energy between the soil, the leaves, and the lower atmosphere. Therefore, a physically sound parameterization similar to those used in the climate models should

be developed based on the physics known at smaller scales, while incorporating important spatial variability in land surface properties.

The Biosphere–Atmosphere Transfer Scheme (BATS; Dickinson et al. 1993) and the Simple Biosphere Schemes (SiB; Sellers et al. 1986) are the most commonly used "big leaf–single soil column" models in global and regional climate studies. Typically, these models solve the energy and water balance equations for only the single soil column and for the big leaf. To characterize the various soil and vegetation properties as well as the hydrological and biogeochemical processes at the earth's surface, these models require a large number of empirical constants that in practice are difficult to estimate. Moreover, there are still unresolved issues as to whether the use of point or small-scale parameters is valid at the atmospheric model grid cell scale. Because these point parameters might vary over an atmospheric model grid cell, it is not clear how these small-scale, local parameters could be aggregated to provide the grid-scale "representative" values that could account for the nonlinearity of the underlying land surface processes (Wood et al. 1992).

To represent the water table dynamics in the land

---

* Current affiliation: Department of Civil Engineering, University of Hong Kong, Hong Kong, China.

Corresponding author address: Dr. Pat J.-F. Yeh, Department of Civil Engineering, University of Hong Kong, Pokfulam Road, Hong Kong, China.
E-mail: patyeh@hkucc.hku.hk

surface parameterization schemes (LSPs) used in climate models, a lumped unconfined aquifer model has been developed and interactively coupled to the land surface transfer scheme (LSX) in a companion paper (Yeh and Eltahir 2005, hereafter Part I). The coupled model is referred to as LSXGW. In Part I, the large-scale groundwater rating curve was estimated empirically using the state-average data in Illinois; however, the impacts of spatial variability were not considered. Since most of the land surface hydrologic processes are nonlinear, the spatial variability of land surface properties would exert significant influences on the large-scale land surface fluxes. In this study, only the subgrid heterogeneity of WTD will be considered since the main focus here is the representation of water table dynamics in LSPs. The strengths of two conceptually different approaches will be combined to account for the subgrid heterogeneity of WTD. After the implementation of the developed subgrid scheme, LSXGW will be tested using data from Illinois for an 11-yr (1984–94) period (as used in Part I). Some remaining significant issues concerning the global parameter estimation will be discussed, and potential solutions to these issues will be suggested.

This paper is organized into five sections. The following section provides a review of the currently available approaches in dealing with the subgrid heterogeneity in LSPs. In section 3, a new methodology combining the strength of the statistical–dynamical (SD) approach and the mosaic approach is proposed and implemented in LSXGW. The test results from the 11-yr (1984–94) simulations in Illinois are presented in section 4. This is followed by the conclusions and the future research suggestions given in section 5.

2. Background

The traditional approach used in BATS and SiB to account for the mixture of surface covers assumes that a single surface cover dominates the entire grid cell. This dominant vegetation type is usually derived by subjective analysis from the available maps or satellite images of land covers. When more than one vegetation coexists within a grid cell, a simple parameter aggregation procedure (most frequently by averaging arithmetically) is employed with respect to the vegetation characteristics to derive a representative, homogeneous mixture of surface types. Note that the traditional approach does not represent different vegetation types simultaneously within a grid cell. Rather, the characteristics of different vegetation types are lumped together into a single effective value. The traditional approach is conceptually less satisfying but computationally more efficient than the mosaic approach. In the following, the

current available approaches in the representation of spatial subgrid heterogeneity are reviewed, and their major strengths and limitations are summarized.

a. Statistical–dynamical approach

The SD approach consists of using probability density functions (PDFs) for describing the various parameters in the soil–vegetation–atmosphere system (see Entekhabi and Eagleson 1989; Avissar 1992). It assumes that land surface characteristics (i.e., vegetation, soil, topography, etc.) or climate forcing (precipitation, temperature, humidity, etc.) vary according to the distributions that can be approximated by continuous analytical PDFs rather than a single representative value. The grid-scale surface fluxes can be calculated using numerical or analytical integration over appropriate PDFs.

Entekhabi and Eagleson (1989) prescribed PDFs to represent the subgrid variability of soil moisture and precipitation. Based on that, the analytical expressions for the runoff, bare soil evaporation, and transpiration were derived. These hydrologic fluxes are calculated not from the grid-scale soil moisture, but from the PDFs of soil moisture and precipitation. However, their determination of the PDFs was based on heuristic arguments rather than the site-specific information. The variability in topography (i.e., elevation) is ignored in their study. Famiglietti and Wood (1991) proposed the use of the TOPMODEL framework to parameterize the spatial variability of soil moisture and the land surface fluxes within a catchment. They used a simple model linking soil moisture to the site-specific soil-topography index (Beven and Kirkby 1979). Only the statistics of the soil-topography index are required as the model input. However, their model has not been implemented in a land surface scheme. Pitman et al. (1990) used an LSP driven by the GCM-generated climate forcing to investigate the impact of the subgrid variability of precipitation on the surface water balance. Similar to Entekhabi and Eagleson (1989), an idealized PDF of precipitation was specified in their work. Wood et al. (1992) present a generalization of the simple bucket model by assigning a statistical distribution of bucket sizes within a grid cell. The Variable Infiltration Capacity (VIC) concept they proposed is defined as the total volumetric capacity of a soil column to hold water. Since the VIC concept is closely related to the saturation excess mechanism, their model is specifically suitable in dealing with the heterogeneity associated with the generation of saturated excess (Dunne-type) runoff, while the treatments in infiltration excess runoff and groundwater runoff (base flow) are overly simplified.

Avissar (1992) proposed a parameterization based on

the SD approach to represent the land surface heterogeneity in numerical atmospheric models. A 25% difference was predicted between the sensible and latent heat fluxes computed with this SD approach and that computed by a "big leaf model. Bonan et al. (1993) used an LSP to examine the influence of subgrid variability in leaf area index, stomata resistance, and soil moisture on the surface energy balance but periodically prescribed a spatially uniform precipitation. Leung and Gahn (1995) proposed a subgrid parameterization of orographic precipitation for the regions with complex topography, by assuming that land surface processes, precipitation, and clouds are all related to the surface elevation. The subgrid variations of surface elevation are aggregated to a limited number of elevation classes, each assigned with vegetation and surface parameters to compute the area-weighted average fluxes. This study has been extended (Leung and Gahn 1998) to include a subgrid vegetation scheme based on the statistical relationship between surface elevation and vegetation. Stieglitz et al. (1997) investigated specifically the importance of topography on the partitioning of surface water and energy fluxes by developing a subgrid parameterization of topography. This scheme uses an analytical form of TOPMODEL equations and the statistics of the topography distribution and then couples with a one-dimensional soil column model to account for the topographic effect.

b. Mosaic approach

The mosaic approach assumes that the different vegetation types within a model grid cell separately exchange momentum, energy, and water mass with the atmosphere. The various vegetation types do not interact with each other but interact vertically with the atmosphere directly above them. This method groups all the vegetation of similar types within a grid cell into a "tile" or "patch." The land surface model calculates separate energy balances for each tile using mean grid cell atmospheric forcing and computes the area-weighted grid-average fluxes of heat, moisture, and momentum.

Avissar and Pielke (1989) was the first study to suggest this modeling approach within a mesoscale atmospheric model, while Koster and Suarez (1992) was the first study to develop the method and implement it in a GCM. Moreover, Seth et al. (1994) presented an approach that explicitly incorporates multiple subgrid heterogeneities of land surface characteristics. Giorgi (1997a, b) proposed a methodology to combine the mosaic and statistical–dynamical approach. A grid cell is divided into fractional areas covered by various surface types. Within each surface type, soil moisture content and surface temperature are assumed to follow continu-

ous analytical PDFs. However, only linear and symmetric PDFs are chosen by the author since their simplicity allows ready analytical integration. Most recently, Koster et al. (2000) developed a catchment-based approach for modeling the land surface processes in GCMs by partitioning continental areas into a mosaic of hydrologic catchments through analysis of surface elevation data. The subgrid heterogeneity of soil moisture was related to topographic characteristics and to bulk soil moisture variables.

c. Discussion

By using the SD approach, complex soil–vegetation–atmosphere representations may not need to be parameterized explicitly. However, depending on how many variables are represented as probability distributions and how many integration intervals are used, this approach can be computationally expensive. Moreover, to apply the SD approach one has to determine a priori the desired probability density functions of certain land surface variables. However, in practice this task is limited by the difficulty of identifying these distributions. Also, the derived functions may be limited to the specific PDFs assumed for the relevant land surface characteristics.

Another difficulty in the use of the SD approach is associated with description of the overlying atmospheric forcing (Seth et al. 1994; Sivapalan and Woods 1995). Since GCM only provides the grid-scale average precipitation, the exact location of precipitation is unknown. The use of a wetting fraction in current LSPs can nominally account for the subgrid variability of precipitation; however, the wetting fraction concept is unable to carry any information on the spatial pattern of precipitation from time step to time step. Because only the grid-mean values of soil moisture or canopy storage are updated for each time step, the detailed information within each subgrid region from the previous time step is lost. As a result, the persistence and amplification of the hydroclimatic anomalies within subgrids cannot be reflected in the SD approach.

The problem discussed above can be avoided by using the mosaic approach. Since unique energy and water budgets are maintained for each subgrid tile in the mosaic approach, there is no loss of memory from one step to the next, and the evolution of prognostics in each subgrid can be traced with consistency. However, given that the typical scale of hydrologic processes is of the order of less than 100 m, significantly more detailed than the scale can be achieved by grid subdivision, the problem of parameter aggregation still exists, but just simply transferred to another scale (Johnson et al. 1992). Moreover, recall that in this approach various subgrids do not interact with each other, which means

the horizontal cross-grid water transport is actually neglected. This transport may become more important as the grid subdivision becomes finer and finer such that a subgrid might not be a closed hydrologic unit. Finally, the mosaic approach not only shares the same computational constraint as the SD approach, but it requires a larger amount of data than the SD approach does. Therefore, the mosaic approach is more useful for offline sensitivity studies, but probably computationally too expensive for use in operational climate models.

3. Subgrid heterogeneity of water table depth

In Part I, an unconfined aquifer model based on water balance computations was developed and interactively coupled to the LSX. The coupled model (LSXGW) has been successfully tested using the 11-yr (1984–94) monthly data from Illinois. However, there are still some disagreements between the LSXGW simulations and the observations probably due to the neglect of subgrid spatial variability of WTD. In this section, a new methodology that combines the SD approach and the mosaic approach will be proposed to incorporate the subgrid heterogeneity of WTD in LSXGW.

Figure 1 shows the long-term (1966–95) average seasonal cycles of the WTD at 15 monitoring wells scattered over Illinois. These 15 wells are all in unconfined conditionsand remote from pumping centers (Yeh et al. 1998). As shown, the average WTD exhibits significant spatial variability among 15 wells with the range from 0 to 15 m below the surface. The objective in this section is to investigate how this small-scale spatial variability can be represented in the LSXGW model, and how it may impact the macroscale hydrological fluxes.

a. The representation of subgrid heterogeneity of WTD in groundwater runoff

In Part I, the unconfined aquifer was represented as a lumped reservoir as follows:

$$S_y \frac{dH}{dt} = I_{gw} - Q_{gw}, \qquad (1)$$

where S_y is the specific yield of the unconfined aquifer, H is the water table level above the datum, I_{gw} is the groundwater recharge flux, and Q_{gw} is the groundwater discharge to streams.

Recall that the observations indicate a strong nonlinear relationship existent between the state-averaged monthly streamflow ($\sim Q_{gw}$) and the corresponding monthly H in Illinois (see Fig. 1 in Part I). It is of interest to investigate whether similar dependence can be observed at the local scale. Figure 2 shows the scatterplots of the 11-yr (1984–94) observed monthly WTD

versus the corresponding nearby streamflow in eight locations of Illinois. The distance between these wells and stream gauges ranges between 5 and 30 km. As seen from this figure, streamflow occurs only when the water table rises above a threshold depth. Similar nonlinear dependence between streamflow and WTD at the local scale has been reported previously (e.g., Senn 1980; Rasmussen and Andreasen 1959). The similar scatterplots (not shown here) of the monthly streamflow versus rainfall in these locations suggest little correlation between them, which together with the correlation shown in Fig. 2 suggests that these streams are predominately fed by the unconfined aquifers. Moreover, an examination of the daily streamflow records in these eight locations reveals that some of these streams are ephemeral, desiccating in summer when the water table is low and connecting with the drainage network during the high water table seasons.

Based on these observations, groundwater runoff at the local scale is formulated as the following threshold-type nonlinear function:

$$
\begin{aligned}
Q_{gw} &= K(d_0 - d_{gw}) \quad \text{if} \quad 0 \le d_{gw} \le d_0 \\
Q_{gw} &= 0 \qquad\qquad\;\; \text{if} \quad d_{gw} \ge d_0
\end{aligned}
\qquad (2)
$$

where d_{gw} (≥ 0) [L] is the water table depth (WTD), K [1/T] is the outflow constant inversely proportional to the aquifer residence time, and Q_{gw} [L/T] is the groundwater runoff. Equation (2) assumes a constant threshold storage, d_0 [L], independent of time, before groundwater runoff occurs. The threshold storage d_0 is a function of the watershed topography relative to the stream network, while the outflow constant K is mainly a function of soil properties.

Also shown in Fig. 2 is the least-absolute-error (LAE) fit of Eq. (2) with respect to the observed WTD and streamflow. The optimal fitting parameters (d_0 and K) for these eight locations are also given in this figure. It was assumed that the magnitude of streamflow is approximately equivalent to that of groundwater runoff in these locations. The best-fit lines are obtained by varying d_0 and K simultaneously within a reasonable range until the optimal values are found that minimize the sum of the absolute errors. Because high streamflow contains more contributions from surface runoff, the LAE criterion is chosen over the commonly used least square error criterion in order to reduce the bias caused by equalizing streamflow to groundwater runoff.

When applying Eq. (1) to a grid cell in climate models (i.e., 100–500 km), H represents the grid-mean water table level. The grid-scale fluxes, I_{gw} and Q_{gw}, cannot be determined solely from the grid-mean WTD because

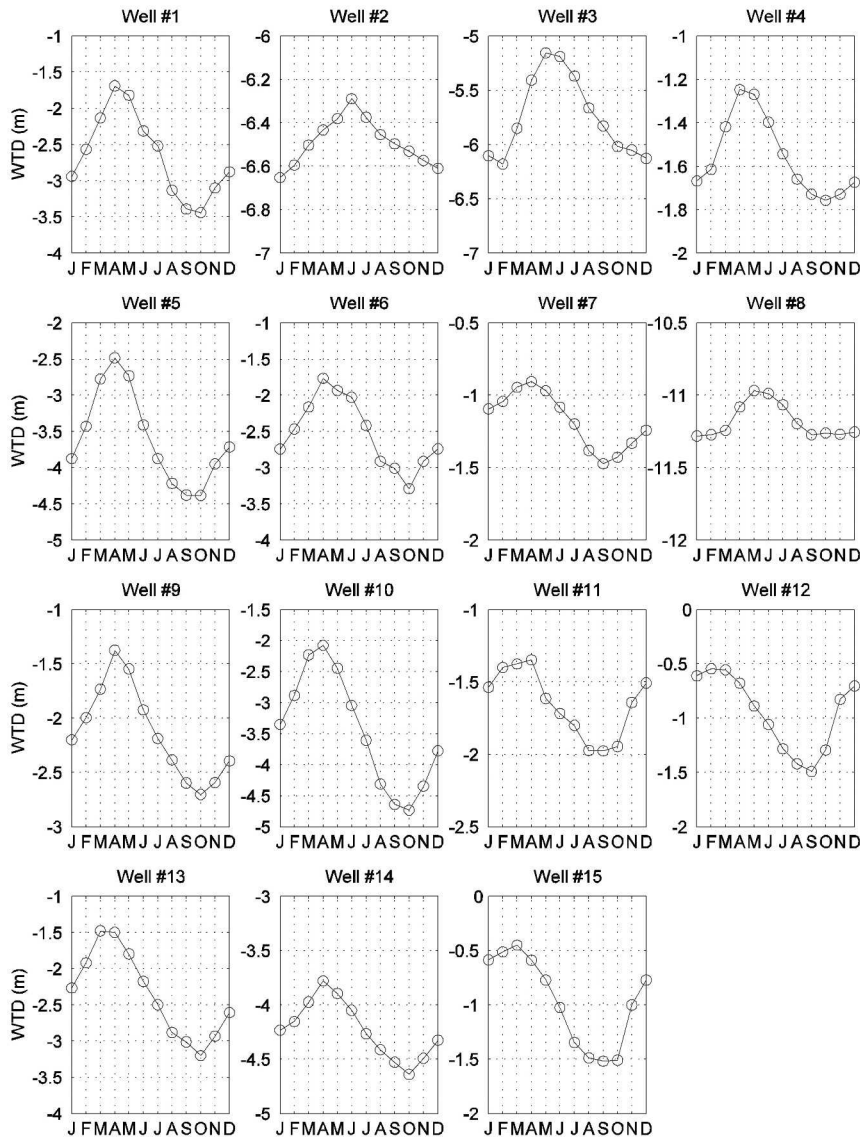LONG-TERM (1966-1995) AVERAGE DEPTH TO WATER TABLE AT 15 WELLS IN ILLINOIS

FIG. 1. Long-term (1966–95) average seasonal cycles of the WTD at 15 monitoring wells located in Illinois.

of the nonlinear dependence between these fluxes and WTD. To overcome this difficulty, an SD approach is proposed to account for the influence of the subgrid heterogeneity of WTD on the grid-scale Q_{gw}. The objective here is to derive the grid-scale groundwater rating curve from using the statistical information on the spatial distribution of WTD. To estimate the spatial distribution of WTD, the histogram of the long-term (1984–94) average d_{gw} at 14 wells in Illinois is plotted in Fig. 3a. Based on this figure, the following two-parameter gamma distribution is assumed to be the PDF of d_{gw}:

$$f(d_{gw}) = \frac{\lambda^{\alpha}}{\Gamma(\alpha)} d_{gw}^{\alpha-1} e^{-\lambda d_{gw}}, \tag{3}$$

where $\Gamma(\alpha)$ is the gamma function; α (shape parameter) and λ (scale parameter) are two parameters related to each other through the grid-mean WTD $E[d_{gw}]$:

$$\lambda = \frac{\alpha}{E[d_{gw}]}. \tag{4}$$

For a given α, the scale of the PDF $f(d_{gw})$ is dynamically shifted based on the time-varying $E[d_{gw}]$. The PDFs for different values of α are plotted in Fig. 3b.

When $\alpha = 1$, the PDF collapses to the exponential distribution. When α approaches infinity, the PDF approaches the Gaussian distribution.

$$E[Q_{gw}] = \int_{d_{gw}=0}^{d_{gw}=d_0} K(d_0 - d_{gw})f(d_{gw})d(d_{gw})$$

$$= \frac{K\lambda^\alpha}{\Gamma(\alpha)}\left\{d_0\left[\frac{(\alpha-1)!}{\lambda^\alpha} - e^{-\lambda d_0}\sum_{k=0}^{\alpha-1}\frac{(\alpha-1)!}{k!}\frac{d_0^k}{\lambda^{\alpha-k}}\right] - \left[\frac{\alpha!}{\lambda^{\alpha+1}} - e^{-\lambda d_0}\sum_{k=0}^{\alpha}\frac{\alpha!}{k!}\frac{d_0^k}{\lambda^{\alpha-k+1}}\right]\right\}. \quad (5)$$

Figure 4 plots $E[Q_{gw}]$ versus $E[d_{gw}]$ for different values of α in comparison with the observed state-average groundwater rating curve. The (grid scale) effective parameters (i.e., $d_0 = 2.64$ m and $K = 0.0393$ month^{-1}) used in Eq. (5) are the arithmetic averages of the eight local-scale parameters shown in Fig. 2. Only the curves for $\alpha = 1$ to 4 are shown in Fig. 4, since as α increases, the sensitivity of the rating curve to α diminishes significantly. As can be observed, the close agreement between the theoretical $E[Q_{gw}]$[Eq. (5), for $\alpha = 3$ or 4] and the observations suggests the suitability of the proposed SD approach in statistically integrating the local-scale groundwater runoff function to the grid-scale groundwater rating curve.

b. The representation of subgrid heterogeneity of WTD in groundwater recharge

In section 3a, the effects of the WTD subgrid heterogeneity in the grid-scale groundwater runoff have been incorporated in the LSXGW by using an SD approach. However, this heterogeneity was not included in the modeling of the unsaturated–saturated zone interactions; namely, the grid-mean WTD was used in the calculation of the groundwater recharge. Since groundwater recharge is a nonlinear function of WTD, the WTD subgrid heterogeneity needs to be accounted for in the calculation of this flux. To explicitly include this effect, a new methodology based on the mosaic approach is proposed in this section.

First, a grid cell is divided into a class of subgrids based on the WTD distribution (see Fig. 5). The areas with a similar WTD are grouped into the same class, say, 0–1 m, 1–2 m, ..., etc. These subgrids coexist within a grid with their individual area fraction variable over time according to the varying grid-mean WTD. Unlike the traditional mosaic approach, these subgrids do not have their absolute geographic locations. The subgrids with a shallow water table are located near the runoff contributing areas, whereas those with a deep water table are located close to the groundwater divide. The fraction of each subgrid varies according to the

The grid-scale groundwater runoff can be derived by integrating the point relationship in Eq. (2) with respect to the PDF of WTD in Eq. (3):

dynamic PDF of WTD [see Eqs. (3) and (4)] and can be determined analytically from the specified PDF. For example, if a grid is divided into three subgrids each with a different WTD ($0 - d_1$, $d_1 - d_2$, and $d_2 - d_3$, respectively), the fractions of each subgrid can be derived as follows:
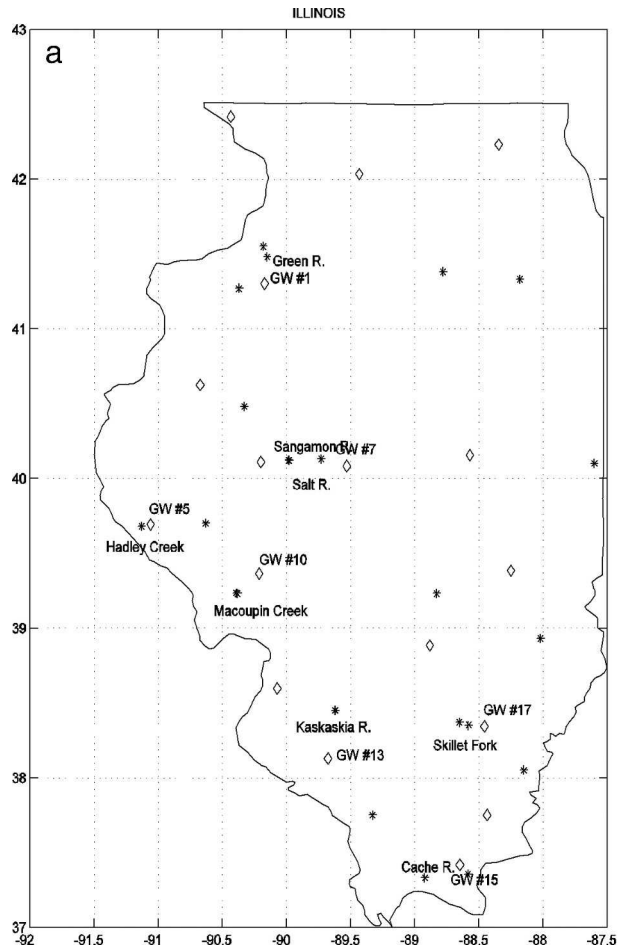

FIG. 2. The scatterplots of the observed monthly WTD vs the corresponding nearby streamflow from 1984 to 1994 in eight locations in Illinois. Also shown in the figure are the optimized parameters (d_0 and K) and the corresponding correlation coefficients derived from the least absolute error criterion.

$$A = A_1 + A_2 + A_3 = \int_{d_{gw}=0}^{d_{gw}=d_3} f(d_{gw})d(d_{gw}) = \frac{\lambda^{\alpha}}{\Gamma(\alpha)}\left[\frac{(\alpha-1)!}{\lambda^{\alpha}} - e^{-\lambda d_3}\sum_{k=0}^{\alpha-1}\frac{(\alpha-1)!}{k!}\frac{d_3^k}{\lambda^{\alpha-k}}\right]$$

$$A_1 = \int_{d_{gw}=0}^{d_{gw}=d_1} f(d_{gw})d(d_{gw}) = \frac{\lambda^{\alpha}}{\Gamma(\alpha)}\left[\frac{(\alpha-1)!}{\lambda^{\alpha}} - e^{-\lambda d_1}\sum_{k=0}^{\alpha-1}\frac{(\alpha-1)!}{k!}\frac{d_1^k}{\lambda^{\alpha-k}}\right]$$

$$A_2 = \int_{d_{gw}=0}^{d_{gw}=d_2} f(d_{gw})d(d_{gw}) - \int_{d_{gw}=0}^{d_{gw}=d_1} f(d_{gw})d(d_{gw});$$

$$A_3 = \int_{d_{gw}=0}^{d_{gw}=d_3} f(d_{gw})d(d_{gw}) - \int_{d_{gw}=0}^{d_{gw}=d_2} f(d_{gw})d(d_{gw}). \tag{6}$$

FIG. 2. (Continued)

FIG. 3. (a) The histogram of the 11-yr (1984–94) average WTD from 15 wells in Illinois; (b) the PDF of a gamma distribution used to fit the histogram of WTD for different values of scale parameters α.

In each time step, each subgrid is simulated independently using the LSXGW. The differences among subgrids are primarily caused by the different water table conditions. The grid-scale hydrological fluxes are computed at the end of each time step by averaging all the subgrid fluxes weighted by their individual fractions. According to the grid-scale fluxes, the grid-mean WTD is updated using Eq. (1) for the next time step.

By using this approach, the dynamic expansion and contraction of the runoff-contributing areas can be simulated explicitly, and the runoff generated from these shallow water table areas can be computed with consistency. Moreover, as a result of the use of the mosaic approach, the spatial distributions of the entire set of hydrological states and fluxes, which are valuable information for the downscaling from the grid scale to the local scale, can be obtained.

4. Simulation results

The results of two offline, 11-yr (1984–94) simulations applying the LSXGW in Illinois (~500 km × 300

km) are presented in this section. The simulation setup, atmospheric input data, the specification of the input soil and vegetation parameters, and the validation data have been described in section 3 of Part I and hence are omitted here. The first simulation uses the version of LSXGW incorporating the effects of WTD subgrid heterogeneity in the grid-scale groundwater runoff (as described in section 3a) and is denoted as "one-column (1-col) simulation" since there is no grid subdivision in this case. In the second simulation, the version of LSXGW incorporating both the SD approach (section 3a) and the mosaic approach (section 3b) is used. In this case, the entire state of Illinois is subdivided into 10 subgrids each with a WTD of 0–1 m, 1–2 m, . . . , 8–9 m, and deeper than 9 m, respectively (as shown in Fig. 5). This is denoted as "10-column (10-col) simulation." These two simulations are designed to demonstrate the respective influences of the WTD subgrid heterogeneity on the groundwater runoff and the groundwater recharge.

Table 1 summarizes the 11-yr (1984–94) mean annual water balance for both the 1-col and the 10-col simulations in comparison with the corresponding observations. Figure 6 plots the annual evaporation ratio (i.e., annual total evaporation/precipitation) and annual runoff ratio (i.e., annual total runoff/precipitation) from 1984 to 1994 for both cases against the observations. According to the observations in Illinois, the 11-yr average annual evaporation and runoff are about 70% and 30% of the average annual precipitation. It can be seen from Table 1 that in general, the partition of the annual precipitation into evaporation and runoff by the LSXGW is fairly well simulated, although the model slightly overestimates evaporation by 20 mm yr^{-1} and underestimates runoff by the same amount. Moreover, the LSXGW successfully reproduces the interannual variability of the annual evaporation and runoff ratios as seen in Fig. 6. Comparing the 1-col case to the 10-col case, two marked differences can be noted (Table 1): 1) For the 10-col case, 24.7% (73.8 mm year^{-1}) of the total runoff is from surface runoff comparing to only 9.1% (27.1 mm year^{-1}) for the 1-col case. 2) The 10-col case simulates 20% less groundwater recharge than the 1-col case. Both of these two differences result from the explicit representation of the shallow water table areas in the 10-col simulation. One great advantage obtained from the grid subdivision in the 10-col case is the provision of realistic soil moisture profile under various water table conditions. Given the fact that most surface runoff in Illinois is generated in the shallow water table areas, explicit grid subdivision is necessary for the realistic simulation of runoff dynamics.
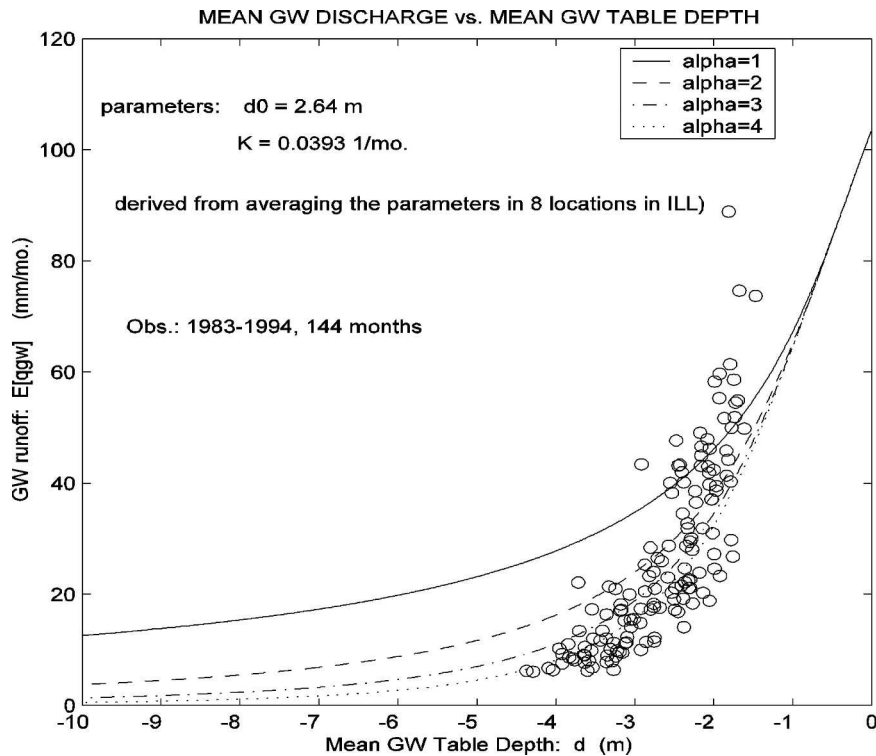
Figure 7 compares the simulated average (1984–94)

MEAN GW DISCHARGE vs. MEAN GW TABLE DEPTH

FIG. 4. Grid-scale groundwater rating curve: the average groundwater runoff ($E[Q_{gw}]$) vs the average WTD ($E[d_{gw}]$) for different values of α. The circles in the figure are the observed state-average groundwater rating curves in Illinois.

seasonal cycles of water table depth, groundwater recharge, and total runoff for both the 1-col and 10-col cases to the corresponding observations. Two major runoff components, groundwater runoff and surface runoff, are also plotted in the figure. Notice that, as stated in Part I, the "observed" groundwater recharge is the estimate from monthly water balance analysis conducted by Yeh (2002) rather than direct observations. Both simulations agree reasonably well with the observations in the timing and the magnitude of the seasonal pattern. However, both simulations fail to capture the peak of groundwater recharge in November when the monthly precipitation is at maximum. As a result, the simulated depth to the water table is unable to fully recover at the end of winter, which eventually leads to the underestimation of streamflow peaks in March and April.

To demonstrate the LSXGW's ability in simulating the interannual variability, the 11-yr monthly time series of the simulated water table depth, groundwater recharge, and total runoff are plotted in Fig. 8 in comparison with the corresponding observations. It can be seen that overall LSXGW faithfully reproduces the interannual variability. In particular, the anomalously low (high) water table level and streamflow during the

drought (flood) year 1988 (1993) are well captured by the LSXGW.

Moreover, the mean seasonal cycle of the total evaporation (i.e., the sum of transpiration, soil evaporation, and interception loss) and the corresponding 11-yr monthly time series are plotted against the observations in Fig. 9. The seasonal cycles of the evaporation simulated in both the 1-col and 10-col cases agree well with the observation except in March. In March, the LSXGW overestimates the evaporation perhaps because of the inaccurate specification of the seasonality of the leaf area index (LAI). Notice that the differences between the simulated evaporation in the 1-col and 10-col cases are unidentifiable, which suggests the WTD subgrid heterogeneity exerts negligible influences on the simulated grid-scale evaporation.

Figure 10 shows the 11-yr mean seasonal cycles of the simulated and the measured soil saturations in each of the 11 soil layers from 0 to 2 m below the surface. It can be observed from this figure that the soil moisture in the surface layers (0–30 cm) experiences insufficient drying during the growing season, while the moisture in the 70–170-cm layers are underestimated up to 10% of the saturation as compared to the measurements. Moreover, 11-yr (1984–94) monthly time series of the
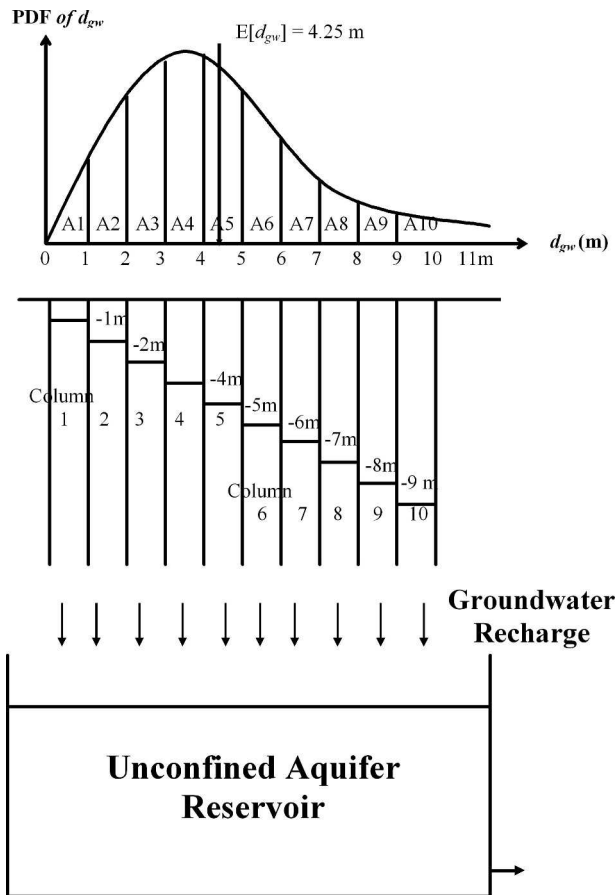
FIG. 5. Schematic representation of the developed multicolumn nonlinear unconfined aquifer model.

proved: 1) the consistent dry bias and the exaggerated amplitude of the soil moisture in the 50–150-cm soil layers and 2) the insufficient drying of the soil moisture in the 0–30 cm during the summers of 1985, 1986, 1989, and 1990.

In summary, by explicitly modeling the water table dynamics and incorporating the subgrid heterogeneity of WTD, most of the hydrological states (soil saturation and water table level) and fluxes (total runoff, evaporation, and groundwater recharge) simulated by LSXGW agree reasonably well with the observations in Illinois. In addition to the long-term climatology, LSXGW also faithfully reproduce the interannual variability of these hydrological variables as evidenced in Figs. 8, 9, and 11. This is encouraging given that only a few assumptions have been made in the model development and no parameter calibration is required in the implementation of LSXGW.

Most of the simulated hydrological variables in the 1-col case and the 10-col case are rather similar. The major explanation for the agreement is that Illinois is a humid area rarely under the water-stressed conditions. The errors in modeling the groundwater recharge using the grid-mean WTD in the 1-col case possibly canceled each other. However, this might not be true for the frequent water-stressed regions in arid climate. On the other hand, the major bias, namely, the overestimation of surface soil moisture in summer, is probably caused by the subgrid heterogeneity of the surface soil moisture. Entekhabi and Eagleson (1989) have shown that by accounting for the subgrid variability of surface soil moisture, the surface runoff increases as a result of its threshold-triggering characteristic. We plan to improve this deficiency by including a subgrid soil moisture scheme in LSXGW in the near future. Another factor that might also be responsible for the overestimated surface soil moisture (as well as the underestimated surface runoff in the col-1 case) is the unrealistic temporal variability of the precipitation forcing (i.e., persistence in wet and dry spells). The temporal statistics (e.g., the average length of wet and dry spells, the total rainy hours percentage, and the mean precipitation intensity conditioned upon rain) of the grid-mean precipitation are significantly distorted by both the spatial and temporal averaging process. The precipitation forcing used in the LSXGW simulations is the average from the observations in more than 100 stations in Illinois. Since the averaging process has significantly smoothed the temporal variability of precipitation in terms of magnitude and frequency, soil moisture is too wet in summer because of the reduced length of dry spells, and surface runoff is too low because of the smoothed rain-

simulated soil water depth in the 0–2-m soil are compared with the observations in Fig. 11. It is encouraging to see that the LSXGW accurately picks up the dry surface soil moisture anomalies in 1988 and 1991, the driest two years during the period 1984–94, which reflects the capability of LSXGW in simulating the surface hydrology under the water-stressed conditions. In addition, the soil moisture in the surface layers during the extremely wet year of 1993 is also well simulated. However, some notable deficiencies need to be im-

TABLE 1. The 11-yr (1984–94) average annual water balance for the LSX 1-column and 10-column simulations in comparison with the corresponding observations: P is precipitation, E is total evaporation, I is groundwater recharge, R is total runoff, Rg is groundwater runoff, and Rs is surface runoff. Units are all in mm yr^{-1}.

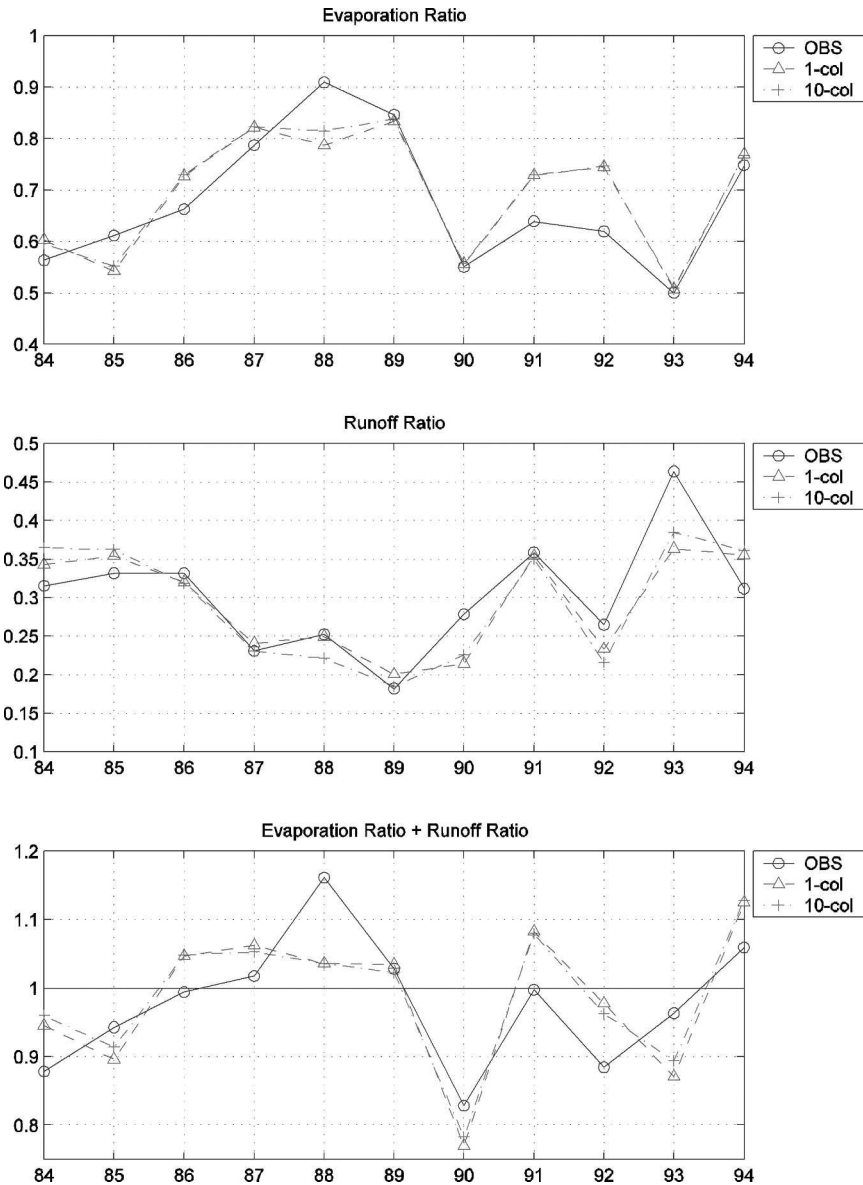|	P	E	I	R	Rg	Rs
Observations	998.5	656.6	253.2	309.3	—	—
1-column simulation	998.5	674.3	264.2	296.9	269.8	27.1
10-column simulation	998.5	677.6	219.2	298.4	224.6	73.8

FIG. 6. The observed and simulated (for both 1-col and 10-col cases) annual evaporation ratio (i.e., annual total evaporation/precipitation) and annual runoff ratio (i.e., annual total runoff/precipitation) from 1984 to 1994.

storm magnitudes. This topic is also currently under research.

It is worthwhile to note from Fig. 6 that the realistic simulation of evaporation in 1993 could not lead to the correct runoff in the same year, and the realistic runoff in 1991–92 could not guarantee the correct evaporation, both of which imply erroneous simulations of the annual changes in the subsurface storages in these years by LSXGW. This emphasizes the importance of the change in the subsurface storage, especially the shallow aquifer storage, in the hydroclimatic simulation at the annual time scale.

A by-product of the 10-col simulation are the spatial distributions of the entire hydrological variables at the subgrid scale. For example, Fig. 12 illustrates the 11-yr mean seasonal cycles of the groundwater recharge and surface runoff. Several interesting behaviors can be noted: 1) The subgrids with a shallow water table have more intensive unsaturated–saturated zone interactions as evidenced by the larger amplitude of the seasonal cycles of groundwater recharge. 2) The groundwater recharge in column 1 (i.e., with the WTD of 0–1 m) is always (negative) upward throughout a year. The magnitude of the upward groundwater fluxes reaches the
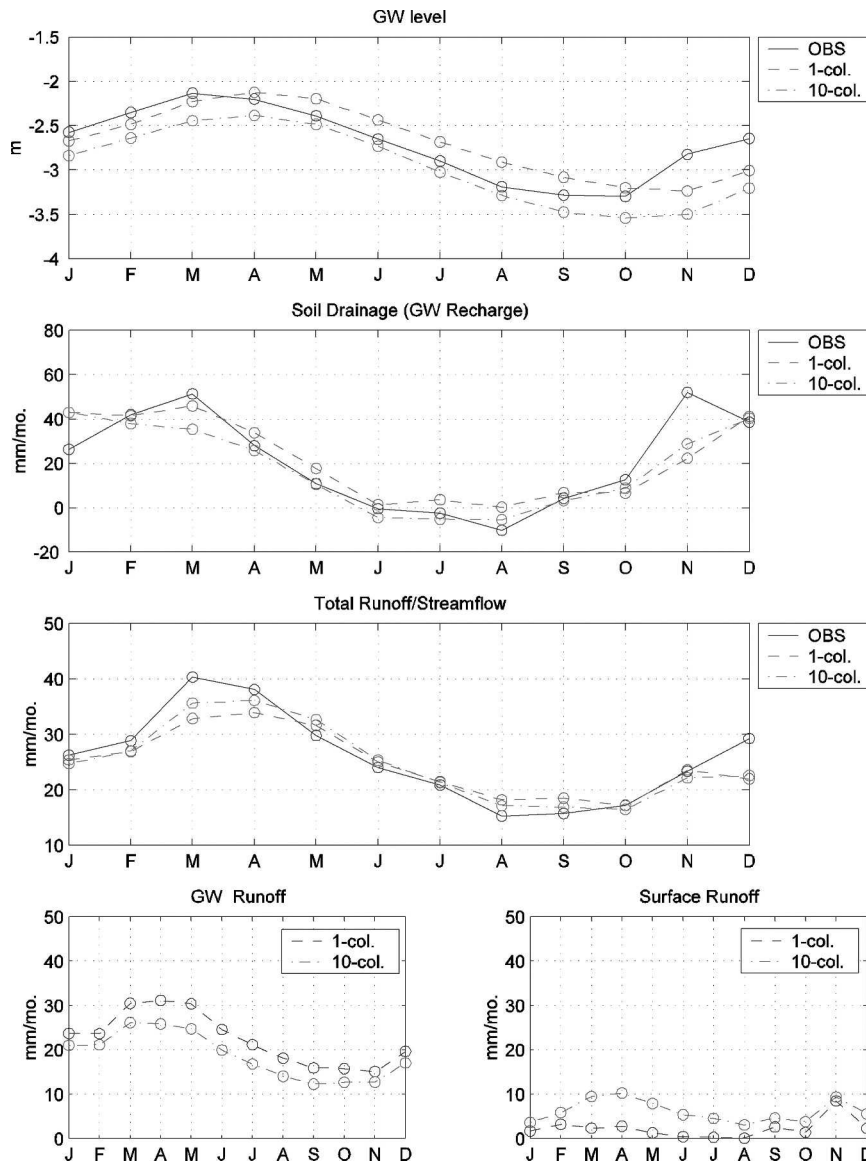
FIG. 7. The 11-yr (1984–94) average seasonal cycles of WTD, soil drainage (groundwater recharge), total runoff, and the two major components of runoff: groundwater runoff and surface runoff.

peak in summer (~100 mm month^{-1}). Other than column 1, upward fluxes occur only during the summer for the subgrids with the WTD shallower than 3 m. 3) Surface runoff is generated almost completely from column 1; other subgrids only produce a negligible amount of surface runoff in November when the precipitation is at a maximum.

To demonstrate the influences of water table position on evaporation, the 11-yr (1984–94) mean seasonal cycles and the 11-yr monthly time series of the total evaporation in each subgrid are plotted in Fig. 13. From this figure, it can be seen that the subgrids with a shal-

low water table (0–3 m) have slightly higher evaporation during the growing season. Also, the differences in evaporation between the shallow WTD subgrids are discernible only during the water-stressed conditions such as in 1988 and 1991. The fact that the shallow water table regions produce a higher evaporation than other regions suggests the groundwater supply to the root zone soil moisture for maintaining the high evapotranspiration rate during the summer, which has been identified as one of the major roles that unconfined aquifers play in the regional hydroclimatology in Illinois (Yeh 2002).
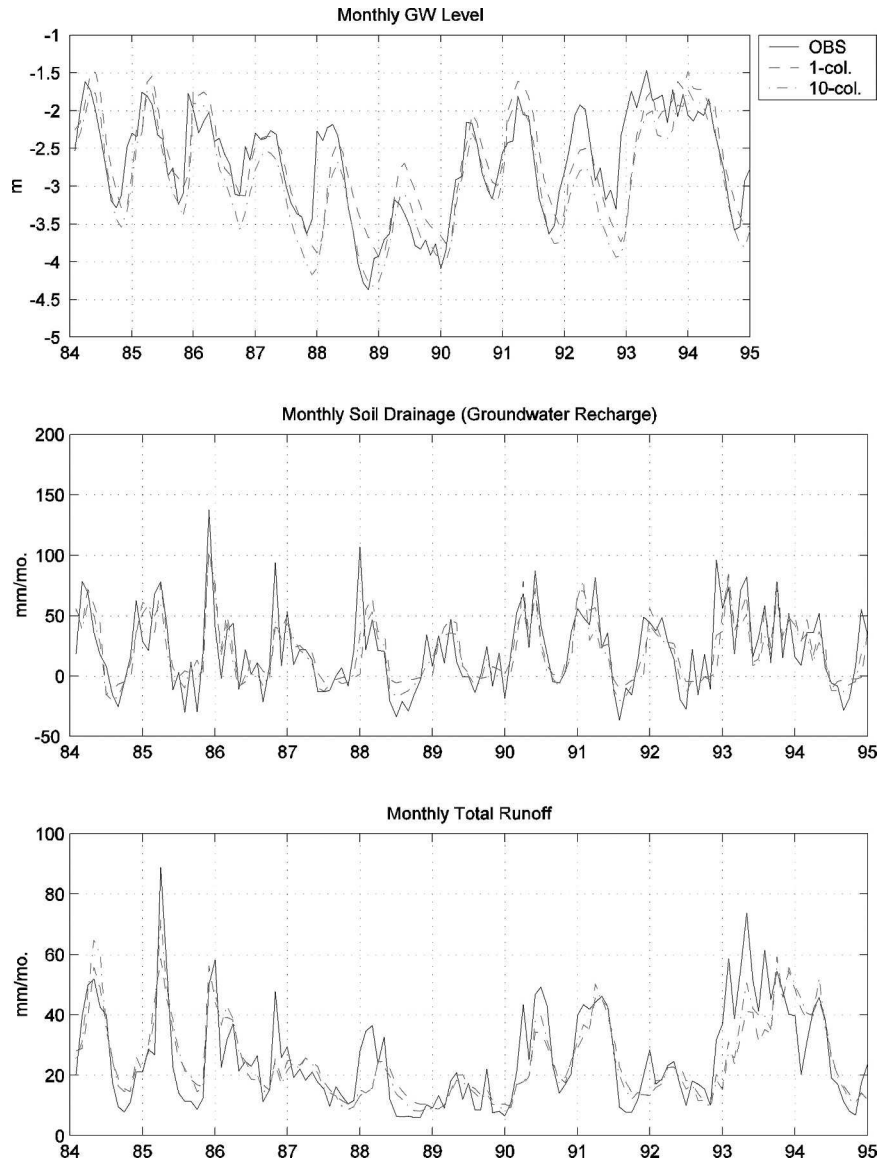
FIG. 8. The simulated 11-yr (1984–94) monthly time series of (a) water table level, (b) groundwater recharge, and (c) total runoff for both 1-col and 10-col cases in comparison with the observations.

Figure 14 plots the 11-yr monthly time series of the area fraction for each of the 10 columns. From this figure, the fraction of shallow (deep) water table area decreases (increases) during the drought year of 1988. The opposite trend can be observed during the flood year of 1993. Therefore, the dynamic expansion and contraction of the shallow water table runoff contributing areas can be explicitly simulated with consistency by the proposed methodology combining the SD and the mosaic approaches.

To investigate the model's response to the water-stressed condition, an 11-yr (1984–94) simulation simi-

lar to the 10-col case was carried out in which the precipitation was reduced 50% with the remaining conditions unchanged. Because of the 50% precipitation, the water table level decreases monotonically during the 11-yr period as a result of the nearly zero groundwater recharge (not shown). The nonlinearity of the hydrological system is significant in that groundwater runoff is only about 25 mm yr^{-1}, which is less than 10% of that generated in the 100% precipitation simulations. Figure 15 shows the 11-yr (1984–94) mean seasonal cycles and the 11-yr monthly time series of the total evaporation in each subgrid for the 50% precipitation simulation. Un-
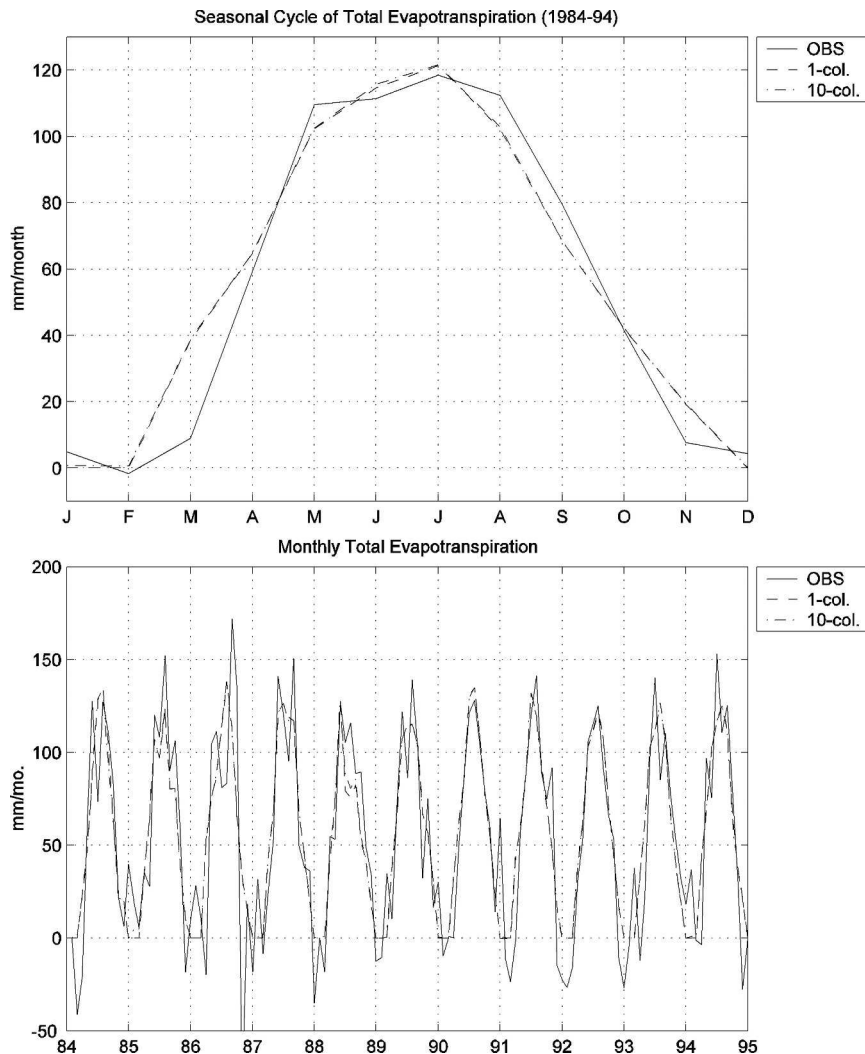
FIG. 9. The 11-yr (1984–94) average seasonal cycle of the observed and simulated total evaporation and the corresponding 11-yr monthly time series.

like the 100% precipitation case (Fig. 13), the differences in the evaporation for the subgrids with WTD of 0–5 m are significant during the growing seasons (May–October). It is interesting to note that even under 50% precipitation condition, the subgrid with shallowest water table (column 1) still produces a high evaporation rate in summer (120 mm month^{-1}). However, the 11-yr mean area fraction of column 1 is less than 1% (due to the 50% precipitation), and therefore the average annual evaporation is much smaller than that in Fig. 13. Moreover, the differences in the simulated evaporation for columns 1–3 are significant in every year except the flood year of 1993, and the differences reach the maximum in the drought year of 1988. By comparing Fig. 15 to Fig. 13, the significance of the shallow unconfined aquifer in supplying water to the root zone soil mois-

ture for evaporation under the water-stressed conditions is underscored.

In summary, the proposed methodology combines the strengths of the SD and the mosaic approaches to account for the subgrid heterogeneity of WTD. It explicitly subdivides a grid into several subgrids based on WTD for the calculation of the grid-scale groundwater recharge, hence the prognostics in each subgrid can be traced with consistency from time step to time step without losing the memory. On the other hand, the model uses a statistical approach to integrate the point groundwater runoff generation function into the grid-scale groundwater rating curve. Since both approaches use an identical form of the PDF of WTD, this combined methodology is consistent in the model framework and easy to implement in the practical applica-
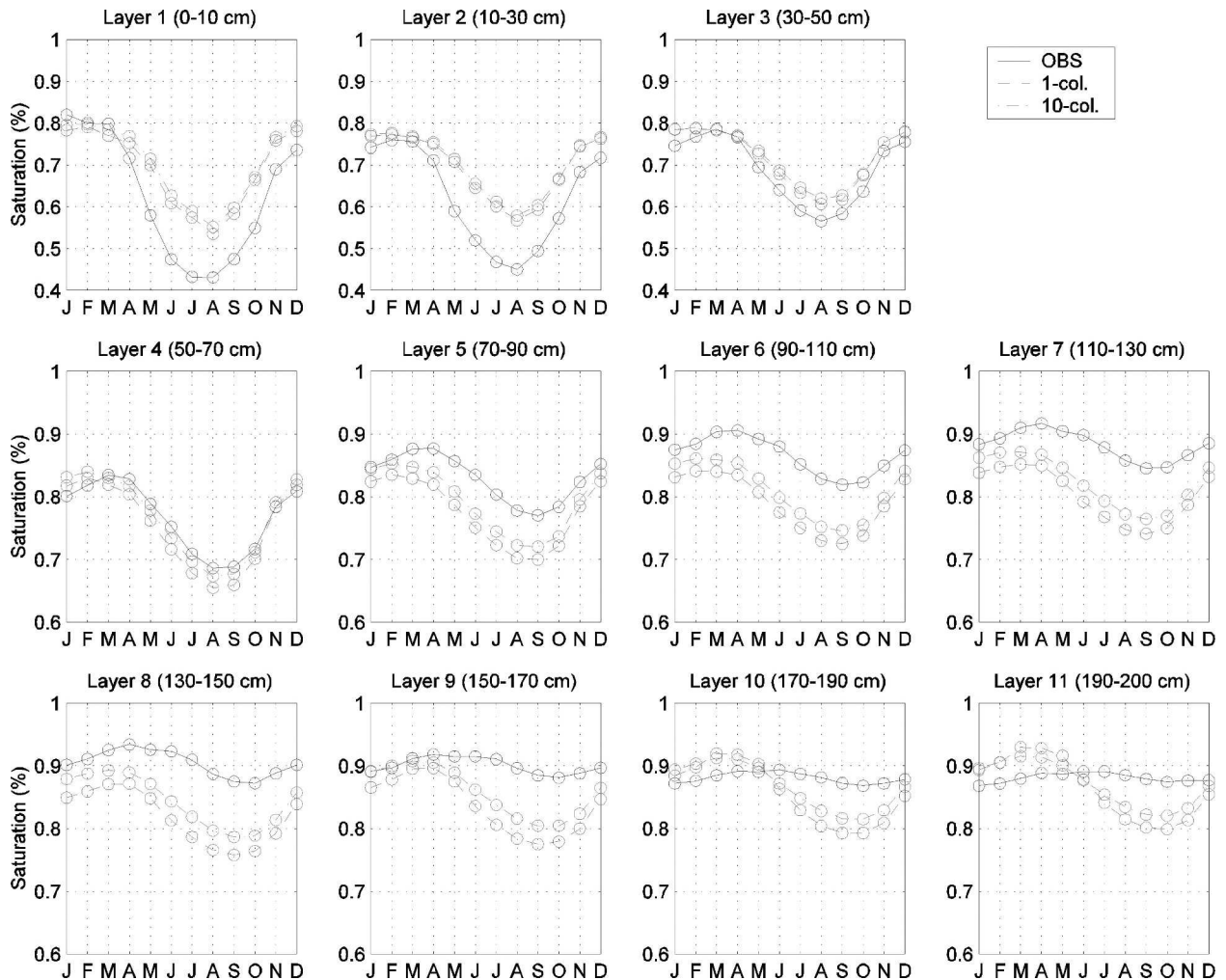
FIG. 10. The 11-yr (1984–94) mean seasonal cycles of the observed simulated soil saturation from 0 to 2 m below the ground surface.

tions. Moreover, only two–four parameters in the aquifer model need to be specified. As a result of the use of analytical expressions in the aquifer model, the computational requirement for the 10-col simulation is still rather economical. Therefore, it can be concluded that the developed model is parsimonious and computationally efficient; thus it is suitable for the use in climate models. Moreover, a valuable by-product is the information on the spatial distributions of the relevant hydrologic quantities at the subgrid scale. This information, which is absent in most of the current LSPs, is valuable in many applications, such as the assessment of the impacts of climate changes on the regional water resources.

5. Concluding remarks

To incorporate the water table dynamics into climate models, a lumped unconfined aquifer model was devel-

oped and interactively coupled to a land surface scheme, LSX (Yeh and Eltahir 2005). This model is parsimonious and computationally efficient; hence it is suitable for the use in climate models. To account for the subgrid heterogeneity of water table depth (WTD), a new methodology, combining the strengths of the statistical–dynamical (SD) approach and the mosaic approach, is proposed in this paper.

First, the point groundwater runoff in LSXGW is parameterized as a threshold-type nonlinear function of WTD based on the local-scale observations in Illinois. A two-parameter gamma distribution is specified as the PDF of WTD. The grid-scale groundwater runoff is derived by statistically integrating the point-scale groundwater runoff function with respect to the PDF of WTD. The resulting groundwater rating curve agrees well with the observations. Next, a grid cell is divided into a class of subgrids based on the WTD in order to
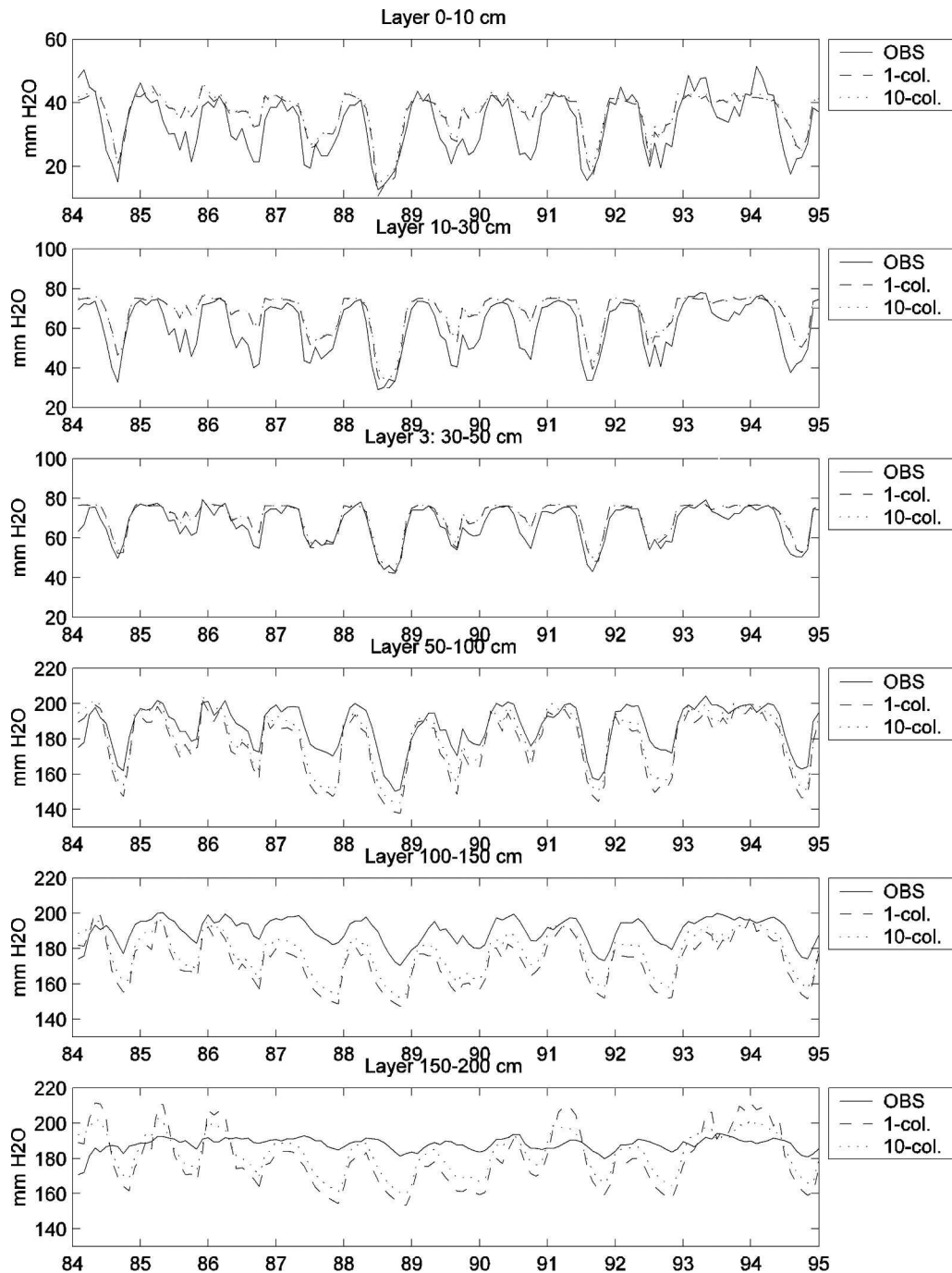
FIG. 11. The 11-yr monthly (1984–94) time series of the simulated soil water depth from 0–2 m below the ground surface.

faithfully model the unsaturated–saturated zone interactions under various water table conditions rather than using the grid-mean WTD in the computation of the grid-scale groundwater recharge. The PDF of WTD, as well as the fraction of each subgrid, varies with time according to the dynamic grid-mean WTD.

The grid-scale hydrological fluxes are computed by averaging the subgrid fluxes weighted by their individual fraction at the end of each time step.

The proposed combined SD–mosaic approach deterministically keeps track of the prognostics in each subgrid in a consistent manner without losing memories

FIG. 12. The 11-yr (1984–94) average seasonal cycles of the (a) groundwater recharge and (b) surface runoff. Column 1 denotes the subgrid with a water table shallower than 1 m below the surface, while column 10 denotes the subgrid with a water table deeper than 9 m.

from step to step, whereas it statistically incorporates the unresolved spatial heterogeneity of WTD within each subgrid. It has the advantage that the dynamic expansion and contraction of the near-stream contributing area can be simulated explicitly without invoking any additional assumptions or parameterizations. Another useful by-product obtained is the availability of the information on the spatial distributions of hydrometeorological variables at the subgrid scale. This in-

formation is useful for the studies of the impacts of climate changes on the regional water resources.

This coupled Groundwater–Soil–Vegetation–Atmosphere Transfer Scheme, called LSXGW, has been tested in Illinois for an 11-yr period from 1984 to 1994. The simulation results indicate that the simulated hydrological states (e.g., water table depth and soil saturation) and fluxes (e.g., groundwater recharge, total runoff, and total evaporation) all have reasonably good
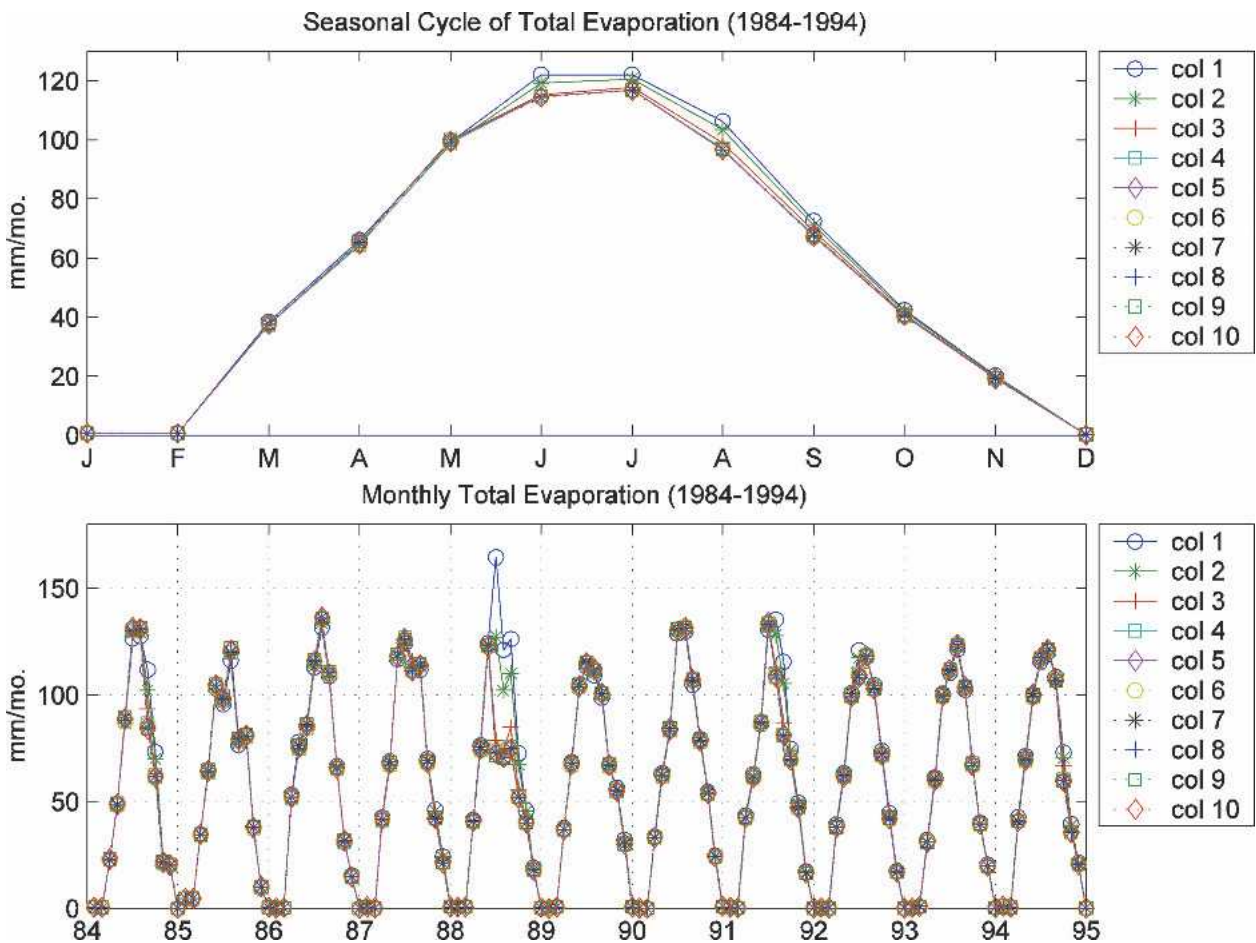
FIG. 13. The 11-yr (1984–94) mean seasonal cycle and the 11-yr monthly time series of the total evaporation in each of the 10 columns.

agreement with the hydrological observations in Illinois.

Comparing the developed LSXGW model to the original LSX, several improvements in the hydrological process representations are significant. From Table 1, it can be seen that the 10-column case generates about 3 times geater surface runoff (73.8 mm year^{-1}) than the 1-column case (27.1 mm year^{-1}). The surface runoff generated by the 1-column model (as well as in the original LSX) is primarily the Hortonian runoff when rainfall exceeds the infiltration capacity. The 10-column model takes a step further to simulate the Dunne-type mechanism (saturation excess runoff). The simultaneous consideration of both Hortonian and Dunne-type mechanisms is largely absent in most current LSPs, except in Entekhabi and Eagleson (1989), Famiglietti and Wood (1991), and Liang and Xie (2001). As stated, the by-product of saturated area fraction shown in Fig. 14 is valuable information in many applications. The absence of saturation excess runoff in current LSPs is

also directly associated with the missing component of water table depth in LSPs. Furthermore, the groundwater contribution to the evapotranspiration in the shallow water table areas may account for a significant portion of total evapotranspiration when the soil moisture deficit is large in summer months. This mechanism has been evidenced from the analysis of Illinois hydrological data (Yeh 2002), and its importance is highlighted in Figs. 13 and 15 of this paper.

However, it should be recognized that the satisfactory performance of the LSXGW in the Illinois simulation is to a large extent attributed to the successful reproduction of the grid-scale groundwater rating curve (see Fig. 6). Specifically, the success stems from the reliable estimation of the required parameters (i.e., d_0 and K) in the aquifer model, namely due to the availability of the data on the water table depth and streamflow in Illinois. It is unrealistic to expect that these data, especially water table observations, are globally available. Since the LSXGW is aimed to be used in climate
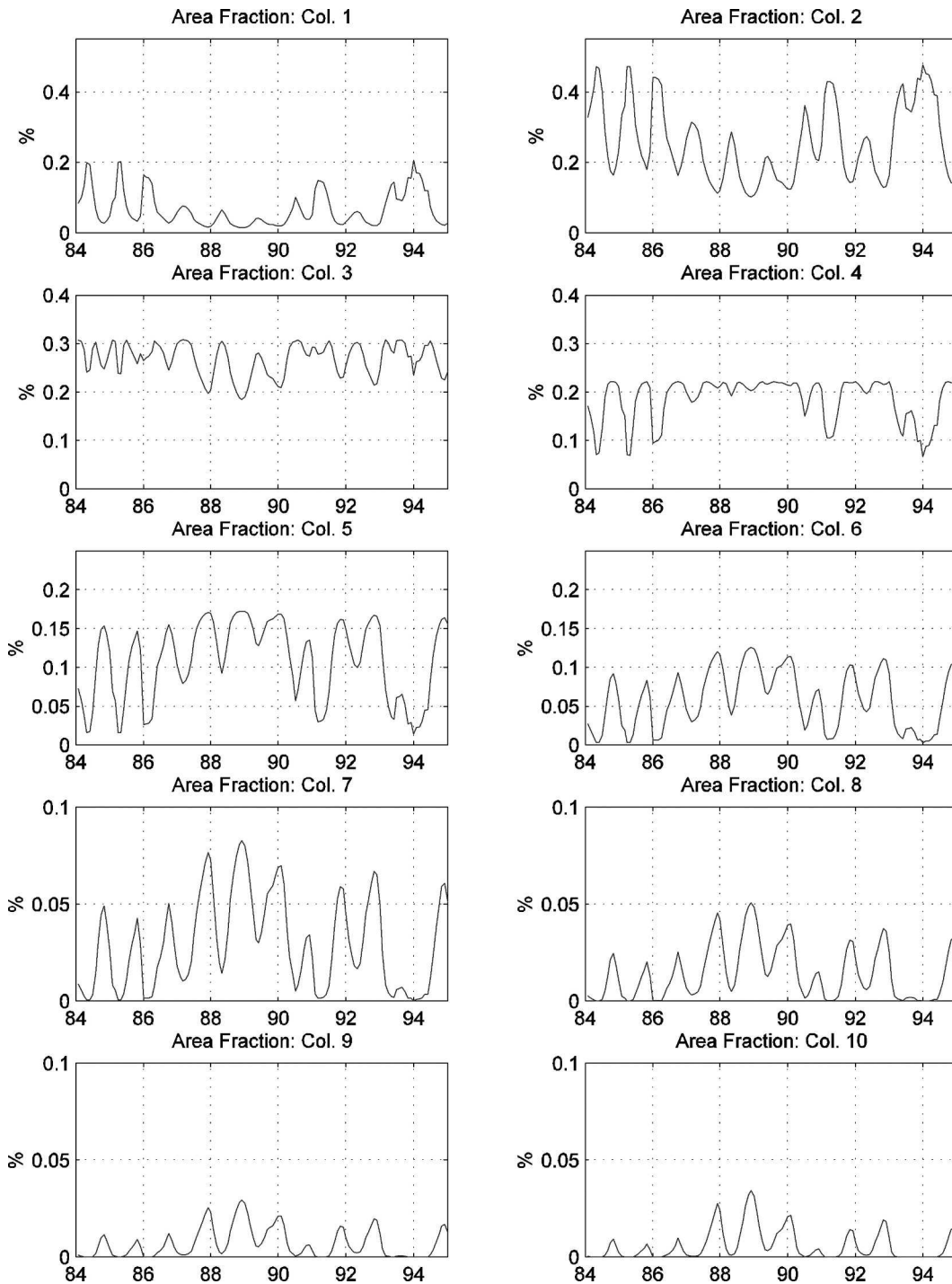
FIG. 14. The 11-yr (1984–94) monthly time series of the area fraction in each of the 10 columns. Column 1 is the area with WTD between 0 and 1 m below the surface; column 2 is the area with WTD between 1 and 2 m below the surface, and so on; column 10 is the area with WTD between 9 and 10 m below the surface.

models, a globally feasible procedure of parameter estimation is undoubtedly the greatest challenge ahead.

A parameter estimation approach using the observed daily streamflow record to calibrate the aquifer param-

eters in the LSXGW has been developed, and its applicability has been demonstrated in several watersheds in Illinois. This approach is similar to Abdulla et al. (1999), who used the daily streamflow data to estimate
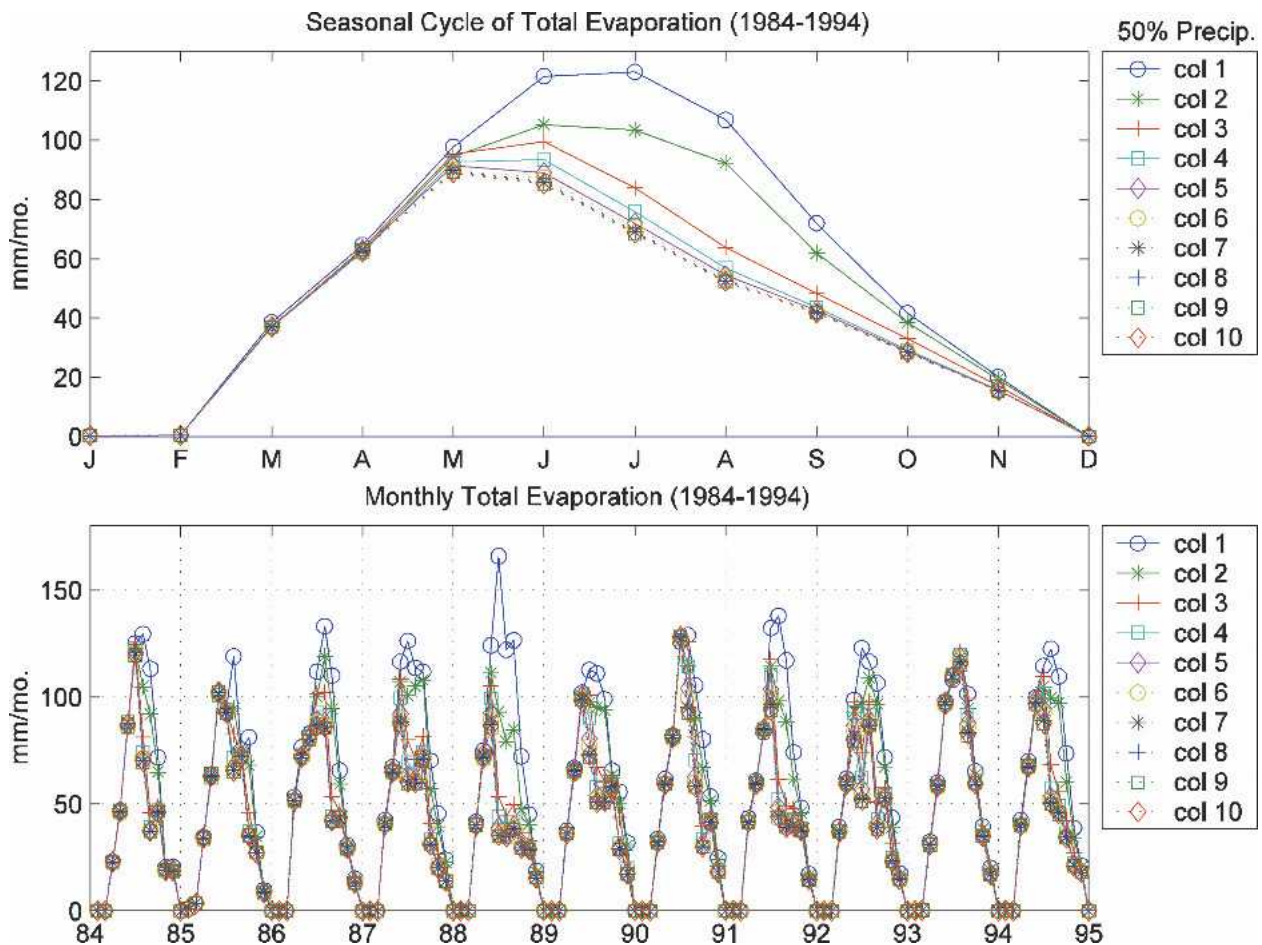
FIG. 15. Same as in Fig. 13, but for the 50% precipitation case 11-yr (1984–94) average seasonal cycle and the 11-yr monthly time series of the total evaporation in each of the 10 columns

the base flow parameters in the ARNO model. Our developed approach is based on the calibration of the simulated daily groundwater runoff against the daily base flow sequences estimated from the digital recursive filter approach (Nathen and McMahon 1990; Chapman 1991; Furey and Gupta 2001). The major groundwater parameters to be calibrated are d_0 and K. The remaining two parameters, the shape parameter α and the specified yield S_y, are found to be not sensitive to the simulation results within their reasonable ranges in this study. In fact, the value of S_y for various soil textures can be found in the literature (e.g., Johnson 1967; Domenico and Schwartz 1990, p. 69). Therefore, only d_0 and K are calibrated in the four test basins in Illinois—the Green River basin, the Cache River basin, the Salt River basin, and the Kaskaskia River basin—without using the local water table depth data in these basins. The results of applying the LSXGW model to and the parameter calibration in these four basins will be presented in a follow-up paper.

Finally, our ongoing research has been focused on developing the grid-based version of the LSXGW model and applying it to the Arkansas–Red River basin as in the Project for Intercomparison of Land Surface Parameterization Scheme Phase 2(c) [PILPS 2(c)], and perhaps to other contrasting environments. It would be worthwhile to first investigate whether the LSXGW model can satisfactorily simulate the hydroclimatology in a water-deficient arid region such as the Sahel in West Africa.

REFERENCES

Abdulla, F. A., D. P. Lettenmaier, and X. Liang, 1999: Estimation of the ARNO model baseflow parameters using daily streamflow data. *J. Hydrol., 222,* 37–54.

Avissar, R., 1992: Conceptual aspects of a statistical-dynamical approach to represent landscape sub-grid-scale heterogeneities in atmospheric models. *J. Geophys. Res., 97,* 2729–2742.

——, and R. A. Pielke, 1989: A parameterization of heterogeneous land surface for atmospheric numerical models and its impacts on regional meteorology. *Mon. Wea. Rev., 117,* 2113–2136.

Beven, K., and M. J. Kirby, 1979: A physically based, variable contributing area model of basin hydrology. *Hydrol. Sci. J., 24,* 43–69.

Bonan, G. B., D. Pollard, and S. L. Thompson, 1993: Influence of subgrid-scale heterogeneity in leaf area index, stomatal resistance, and soil moisture on grid-scale land–atmosphere interactions. *J. Climate, 6,* 1882–1897.

Chapman, T. G., 1991: Comment on "Evaluation of automated techniques for base flow and recession analyses" by R. J. Nathan and T. A. McMahon. *Water Resour. Res., 27,* 1783–1784.

Dickinson, R. E., A. Henderson-Sellers, and P. J. Kennedy, 1993: Biosphere-Atmosphere Transfer Scheme (BATS) version 1e as coupled to the NCAR Community Climate Model. NCAR Tech. Note TN-387+STR, 72 pp.

Domenico, P. A., and F. W. Schwartz, 1990: *Physical and Chemical Hydrogeology.* 2d ed. John Wiley & Sons, 824 pp.

Entekhabi, D., and P. Eagleson, 1989: Land surface hydrology parameterization for atmospheric general circulation models including subgrid scale spatial variability. *J. Climate, 2,* 816–831.

Famiglietti, J., and E. Wood, 1991: Evapotranspiration and runoff from large area: Land surface hydrology for atmospheric general circulation models. *Land Surface–Atmospheric Interactions for Climate Models: Observations, Models, and Analyses,* E. Wood, Ed., Kluwer Academic, 179–204.

Furey, P. R., and V. K. Gupta, 2001: A physically based filter for separating base flow from streamflow time series. *Water Resour. Res., 37,* 2709–2722.

Giorgi, F., 1997a: An approach for the representation of surface heterogeneity in land surface models. Part I: Theoretical framework. *Mon. Wea. Rev., 125,* 1885–1899.

——, 1997b: An approach for the representation of surface heterogeneity in land surface models. Part II: Validation and sensitivity experiments. *Mon. Wea. Rev., 125,* 1900–1919.

Johnson, A. I., 1967: Specific yield—Compilation of specific yields for various materials. U.S. Geological Survey Water Supply Paper 1662-D, 74 pp.

Johnson, K. D., D. Entekhabi, and P. Eagleson, 1992: The implementation and validation of improved landsurface hydrology

in an atmospheric general circulation model. Rep. 11, Center for Global Change Science, MIT, 64 pp.

Koster, R. D., and M. J. Suarez, 1992: Modeling the land surface boundary in climate models as a composite of independent vegetation stands. *J. Geophys. Res., 97,* 2697–2715.

——, ——, A. Ducharne, P. Kumar, and M. Stieglitz, 2000: A catchment-based approach to modeling land surface processes in a general circulation model, 1. Model structure. *J. Geophys. Res., 105* (D20), 24 809–24 822.

Leung, L. R., and S. J. Ghan, 1995: A sub-grid parameterization of orographic precipitation. *Theor. Appl. Climatol., 52,* 95–118.

——, and ——, 1998: Parameterizing subgrid orographic precipitation and surface cover in climate models. *Mon. Wea. Rev., 126,* 3271–3291.

Liang, X., and Z. Xie, 2001: A new surface runoff parameterization with subgrid-scale soil heterogeneity for land surface models. *Adv. Water Resour., 24,* 1173–1193.

Nathan, R. J., and T. A. McMahon, 1990: Evaluation of automated techniques for baseflow and recession analysis. *Water Resour. Res., 26,* 1465–1473.

Pitman, A. J., A. Henderson-Sellers, and Z.-L. Yang, 1990: Sensitivity of regional climates to localized precipitation in global models. *Nature, 346,* 734–737.

Rasmussen, W. C., and G. E. Andreasen, 1959: Hydrologic budget of the Beaverdam Creek Basin, MD. U.S. Geological Survey Water Supply Paper 1472, 106 pp.

Sellers, P. J., Y. Mintz, Y. C. Sud, and A. Dalcher, 1986: A simple biosphere model (SiB) for use within general circulation models. *J. Atmos. Sci., 43,* 505–531.

Senn, R. B., 1980: A nonlinear reservoir lumped parameter model for the Herkenhoff farm located near San Acacia. New Mexico Institute of Technology, 80 pp.

Seth, A., F. Giorgi, and R. E. Dickinson, 1994: Simulating fluxes from heterogeneous land surfaces: Explicit sub-grid method employing the biosphere–atmosphere transfer scheme (BATS). *J. Geophys. Res., 99,* 18 651–18 667.

Sivapalan, M., and R. A. Woods, 1995: Evaluation of the effects of general circulation models' sub-grid variability and patchiness of rainfall and soil moisture on land surface water fluxes. *Scale Issues in Hydrological Modeling,* J. D. Kalma and M. Sivapalan, Eds., John Wiley and Sons, 453–473.

Stieglitz, M., D. Rind, J. Famiglietti, and C. Rosenzweig, 1997: An efficient approach to modeling the topographic control of surface hydrology for the regional and global climate modeling. *J. Climate, 10,* 118–137.

Wood, E. F., D. P. Lettenmaier, and V. G. Zartarian, 1992: A land-surface hydrology parameterization with sub-grid variability for general circulation models. *J. Geophys. Res., 97* (D3), 2717–2728.

Yeh, P. J.-F., 2002: Representation of water table dynamics in a land surface scheme: Observations, models, and analyses. Ph.D. dissertation, Dept. of Civil and Environmental Engineering, Massachusetts Institute of Technology, 212 pp.

——, and E. A. B. Eltahir, 2005: Representation of water table dynamics in a land surface scheme. Part I: Model development. *J. Climate, 18,* 1861–1880.

——, M. Irizarry, and E. A. B. Eltahir, 1998: Hydroclimatology of Illinois: A comparison of monthly evaporation estimates based on atmospheric water balance and soil water balance. *J. Geophys. Res., 103* (D16), 19 823–19 837.